

EQUATORIAL BELT OF TITAN REVISITED USING A COMPREHENSIVE RADIATIVE TRANSFER MODEL.

J. F. Brossier¹, S. Rodriguez², L. Maltagliati³, T. Cornet², A. Lucas², S. Le Mouélic⁴, A. Solomonidou^{3,5}, A. Coustenis³, M. Hirtzig^{3,6}, R. Jaumann¹, K. Stephan¹, and R. H. Brown⁷. ¹Institute of Planetary Research, German Aerospace Center (DLR), Berlin, Germany (Jeremy.Brossier@dlr.de). ²Laboratoire Astrophysique, Instrumentation et Modélisation (AIM), Université Paris-Diderot, CEA-Saclay, Gif-sur-Yvette, France. ³Laboratoire d'études spatiales et d'instrumentation en astrophysique (LESIA), Paris-Meudon, France. ⁴Laboratoire de Planétologie et Géodynamique, Université of Nantes, France. ⁵Jet Propulsion Laboratory, California Institute of Technology, Pasadena, CA, USA. ⁶Fondation "La main à la pâte", Montrouge 75006, France. ⁷Lunar and Planetary Laboratory, Univ. Arizona, Tucson, USA.

1. Introduction

After twelve years of exploration, near-infrared imaging data provided from the Visual and Infrared Mapping Spectrometer (VIMS) onboard Cassini [1] reveal a variety of surface units that are compositionally and/or structurally distinct [2,3]. The analysis of the infrared signature of these units enables constraining the surface composition of Titan, which is of prime importance for modelling Titan's interior, surface, and atmosphere, particularly in the search for an endogenic methane source. For this study, we investigate a selection of regions of interest seen in VIMS data by applying methods of correction for the atmospheric contributions.

2. Methods

Because of the dense and absorbent atmosphere of Titan, its surface is only visible in a few narrow atmospheric windows of the near-infrared range centered at 0.93, 1.08, 1.27, 1.59, 2.01, 2.7-2.8 and 5 μm , where the methane absorption is weaker [4]. Nevertheless, these windows still suffer from strong haze scattering and hence different methods of correction were used to remove these atmospheric effects: an empirical correction [5,6] for mapping (and identification) purposes, and a comprehensive radiative transfer model [7-9] in order to retrieve the real surface albedo of our regions of interest. SAR swaths from the RADAR instrument were also used for geomorphological mapping purposes.

3. Regions of Interest

We focus our investigations on several regions located in the equatorial belt ($\pm 40^\circ$), where several geological features have been identified (figure 1) such as: (1)

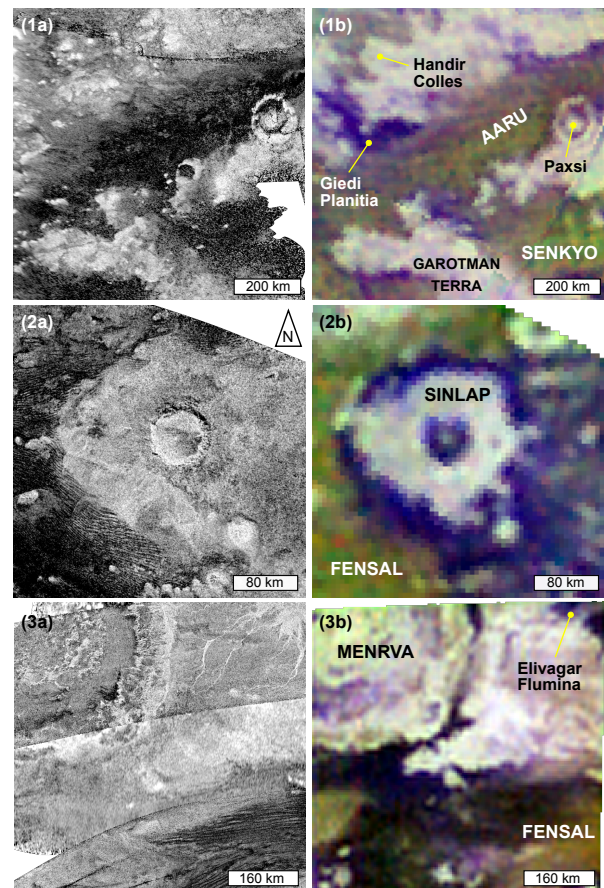


Figure 1. 3 regions of interest investigated in this work: (1) Aaru Regio, (2) Sinlap crater, and (3) Menrva crater. These regions are displayed through (a) mosaics of SAR swaths provided by the RADAR instrument, and (b) false-color composites VIMS with a color scheme of ratios of channels (red: 1.59/1.27 μm , green: 2.01/1.27 μm , and blue 1.27/1.08 μm) after using an empirical correction for the atmospheric contributions. Giedi Planitia is a non-official name for an IR-blue area in Aaru Regio. [North on top]

Aaru Regio (350°W , 5°N), (2) Sinlap crater and its surroundings (16.1°W , 11.3°N), and (3) Menrva crater with Elivagar Flumina (87.2°W , 20.1°N). In this work we used VIMS observations targeting each region

with suitable viewing geometries for the use of our radiative transfer model (meaning incidence and emergence angles $< 60^\circ$).

4. Spectral units' distinction

By using our radiative transfer model, we estimate the surface albedo of our regions of interest for different infrared (IR) units; such as (1) IR-bright units (including plateaus and main ejecta blankets), (2) IR-brown areas corresponding to dunes seen in SAR swaths [10], and (3) IR-blue areas devoid of dunes and supposedly enriched in water ice [11,12]. For reference, we compare our values with those of surface candidates, starting with pure water ice and tholins. Synthetic spectra are computed based on the formalism developed by [13,14]. Surface albedo's spectra reveal different behaviors in the shorter wavelengths (below $2 \mu\text{m}$), suggesting that the 3 IR-units are spectrally distinct in term of composition and/or structure (particles size) (figure 2). Spectral units tend to draw a consistent trend in which the IR-blue materials are strongly fitted with the water ice. Whereas, IR-bright units reveal a lack in coarse water ice and might be covered by a layer of organic sediments (tholins). As for the IR-brown, it seems that the dunes material consists in a granular mixture between water ice and possibly tholins [10], the composition of which will be infer after applying mixing models to our pure spectral endmembers in the near future.

5. Conclusion and Perspectives

This method of analysis allows constraining the compositional and structural relations between the different spectral units. Our results reveal a consistent trend for each spectral units, even between the different regions of interest, but also between several observations targeting these same regions, as recently shown with the regions of Sinlap [15] and Aaru [16]. IR-blue areas seen near the impact craters can be associated to icy particles derived from excavated substrate material that are deposited after the impact [17]. Whereas those found within IR-bright plateaus should correspond to the icy substrate outcropping as mountains (or SAR-rough areas) after being strongly eroded. Then, erosion products (including icy material and organic sand) are transported via channels and washed out at the edge of the IR-bright plateaus,

leading to IR-blue areas, and followed by the IR-brown dunes [18]. This study leads us to connect the possible composition of the spectral units with their geomorphological/geological context. Nonetheless, some improvements of the radiative transfer model are necessary since the longer wavelengths of the near-infrared range ($2.7\text{-}2.8$ and $5.0 \mu\text{m}$) are not used in this work. Indeed, a better knowledge concerning the atmospheric gases and aerosols behaviors in this range should enhance the robustness of our results.

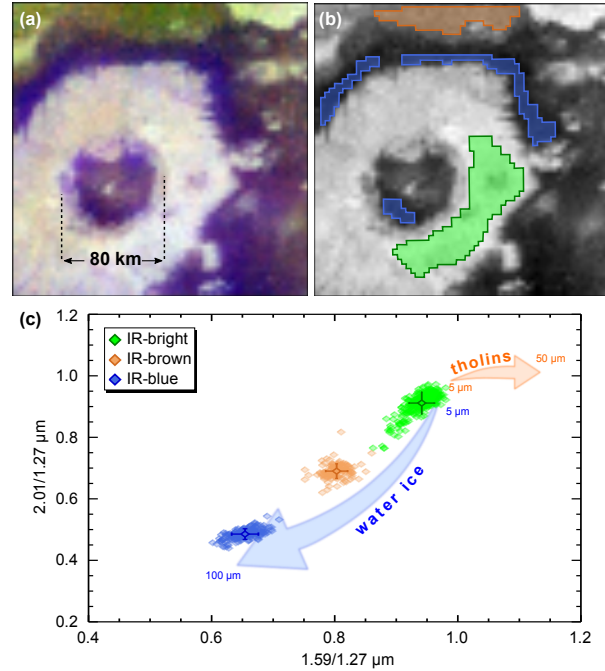


Figure 2. VIMS observation used by the radiative transfer code for Sinlap crater through CM_1805209469 acquired during flyby T110 (March 2015). This empirically corrected observation is non-projected and displayed as (a) false-color composite of ratios of channels (red: $1.59/1.27 \mu\text{m}$, green: $2.01/1.27 \mu\text{m}$, and blue: $1.27/1.08 \mu\text{m}$), and (b) a ratio of $2.01/1.27 \mu\text{m}$. Color-coded masks show the locations where surface albedo values were extracted for the IR-bright units (green plots), IR-brown dunes (brown plots), and IR-blue materials (blue plots), and used for (c) comparison of the $1.59/1.27 \mu\text{m}$ vs $2.01/1.27 \mu\text{m}$ spectral slopes. [North on top]

References

- [1] Brown, R. H. et al. (2005) *SSR*. [2] Barnes, J. W. et al. (2007a) *Icarus*, 186. [3] Soderblom, L. A. et al. (2007) *PSS*, 55. [4] Sotin, C. et al. (2005) *Nature*, 435. [5] Cornet, T. et al. (2012) *Icarus*, 218. [6] Le Mouélic, S. et al. (2012), *PSS*, 73. [7] Hirtzig, M. et al. (2013) *Icarus*, 226. [8] Solomonidou, A. et al. (2014) *JGR*, 119. [9] Maltagliati, L. et al. (2015) *EPSC*. [10] Rodriguez, S. et al. (2013) *Icarus*, 230. [11] Rodriguez, S. et al. (2006) *PSS*, 54. [12] Jaumann, R. et al. (2008) *Icarus*, 197. [13] Hapke, B. (1993) *Cambridge Uni. Press*. [14] Hapke, B. (1993) *Cambridge Uni. Press*. [15] Brossier, J. F. et al. (2016a) *EGU*. [16] Brossier, J. F. et al. (2016b) *DPS*. [17] Le Mouélic, S. et al. (2008), *JGR*, 113. [18] Barnes, J. W. et al. (2007b) *JGR*, 112.